J|A|C|S ARTICLES

Published on Web 12/10/2010

Hangman Corroles: Efficient Synthesis and Oxygen Reaction Chemistry

Dilek K. Dogutan,[†] Sebastian A. Stoian,[‡] Robert McGuire, Jr.,[†] Matthias Schwalbe,[§,†] Thomas S. Teets,[†] and Daniel G. Nocera*[,†]

Department of Chemistry, 6-335, Massachusetts Institute of Technology 77 Massachusetts Avenue, Cambridge, Massachusetts 02139-4307, United States, and Department of Chemistry, Carnegie Mellon University Mellon Institute Pittsburgh, Pennsylvania 15213, United States

Received October 2, 2010; E-mail: nocera@mit.edu

Abstract: The construction of a new class of compounds—the hangman corroles—is provided efficiently by the modification of macrocyclic forming reactions from bilanes. Hangman cobalt corroles are furnished in good yields from a one-pot condensation of dipyrromethane with the aldehyde of a xanthene spacer followed by metal insertion using microwave irradiation. In high oxidation states, X-band EPR spectra and DFT calculations of cobalt corrole axially ligated by chloride are consistent with the description of a Co(III) center residing in the one-electron oxidized corrole macrocycle. These high oxidation states are likely accessed in the activation of O−O bonds. Along these lines, we show that the proton-donating group of the hangman platform works in concert with the redox properties of the corrole to enhance the catalytic activity of O−O bond activation. The hangman corroles show enhanced activity for the selective reduction of oxygen to water as compared to their unmodified counterparts. The oxygen adduct, prior to oxygen reduction, is characterized by EPR and absorption spectroscopy.

Introduction

The hangman construct allows for precise control of the placement of a proton-donating or -accepting moiety over the face of a macrocyclic redox site.[1,2] Bond-making and bond-breaking catalysis of small-molecule substrates residing in the hangman cleft may be activated by proton-coupled electron transfer (PCET)[1−6] where proton transfer is delivered from the hanging group and the redox equivalents and electron transfer is to the macrocycle.[7] The hangman motif heretofore has emphasized porphyrin[8−11] and salen[12,13] macrocycles. We expand the scope of the hangman construct by now reporting the synthesis of a new class of compounds—hangman corroles.

Metallocorrole complexes are relatives of the corrin macrocycle found in coenzyme B12 and they are active catalysts for a variety of transformations.[14,15] Compared to porphyrins, corroles lack one meso bridge carbon atom and thus have a smaller macrocyclic cavity. Moreover, their four nitrogens bear three protons, as compared with two protons in porphyrins. The higher charge of the macrocyclic core, together with electronic considerations, permit corroles to stabilize metals in higher oxidation states,[14,16] and thus open new avenues for oxidative catalysis, especially involving substrates of energy consequence such as carbon dioxide,[17,18] oxygen[19,20] and water.[21] Many of these transformations involve the coupling of the proton to the electron and hence this class of catalysts can benefit from the hangman motif.

The synthesis of variously substituted corroles may proceed along many routes.[22] Recently, corroles have been introduced into Pacman motifs, in which a difunctionalized polycyclic

[†] Massachusetts Institute of Technology.
[‡] Carnegie Mellon University Mellon Institute Pittsburgh.
[§] Current address: Department of Chemistry, Humboldt Universität zu Berlin, Brook-Taylor-Strasse 2, 12489, Berlin.

(1) Rosenthal, J.; Nocera, D. G. *Acc. Chem. Res.* **2007**, *40*, 543–553.
(2) Rosenthal, J.; Nocera, D. G. *Prog. Inorg. Chem.* **2007**, *55*, 483–544.
(3) Chang, C. J.; Chang, M. C. Y.; Damrauer, N. H.; Nocera, D. G. *Biochim. Biophys. Acta* **2004**, *1655*, 13–28.
(4) Nocera, D. G. *Inorg. Chem.* **2009**, *48*, 10001–10017.
(5) Dempsey, J. L.; Esswein, A. J.; Manke, D. R.; Rosenthal, J.; Soper, J. D.; Nocera, D. G. *Inorg. Chem.* **2005**, *44*, 6879–6892.
(6) Reece, S. Y.; Hodgkiss, J. M.; Stubbe, J.; Nocera, D. G. *Phil. Trans. R. Soc. B* **2006**, *361*, 1351–1364.
(7) Chang, C. J.; Chng, L. L.; Nocera, D. G. *J. Am. Chem. Soc.* **2003**, *125*, 1866–1876.
(8) Chng, L. L.; Chang, C. J.; Nocera, D. G. *Org. Lett.* **2003**, *5*, 2421–2424.
(9) McGuire, R., Jr.; Dogutan, D. K.; Teets, T. S.; Suntivich, J.; Shao-Horn, Y.; Nocera, D. G. *Chem. Sci.* **2010**, *1*, 411–414.
(10) Chang, C. J.; Yeh, C.-Y.; Nocera, D. G. *J. Org. Chem.* **2002**, *67*, 1403–1406.
(11) Yeh, C.-Y.; Chang, C. J.; Nocera, D. G. *J. Am. Chem. Soc.* **2001**, *123*, 1513–1514.
(12) Liu, S.-Y.; Nocera, D. G. *J. Am. Chem. Soc.* **2005**, *127*, 5278–5279.
(13) Yang, J. Y.; Bachmann, J.; Nocera, D. G. *J. Org. Chem.* **2006**, *71*, 8706–8714.
(14) Aviv-Harel, I.; Gross, Z. *Chem.—Eur. J.* **2009**, *15*, 8382–8394.
(15) Aviv, I.; Gross, Z. *Chem. Commun.* **2007**, 1987–1999.
(16) Gross, Z.; Gray, H. B. *Comm. Inorg. Chem.* **2006**, *27*, 61–72.
(17) Grodkowski, J.; Neta, P.; Fujita, E.; Mahammed, A.; Simkhovich, L.; Gross, Z. *J. Phys. Chem. A* **2002**, *106*, 4772–4778.
(18) Okamoto, A.; Nakamura, R.; Osawa, H.; Hashimoto, K. *J. Phys. Chem. C* **2008**, *112*, 19777–19783.
(19) Kadish, K. M.; Shen, J.; Fremond, L.; Chen, P.; Ojaimi, M. El.; Chkounda, M.; Gros, C. P.; Barbe, J.-M.; Ohkubo, K.; Fukuzumi, S.; Guilard, R. *Inorg. Chem.* **2008**, *47*, 6726–6737.
(20) Kadish, K. M.; Fremond, L.; Shen, J.; Chen, P.; Ohkubo, K.; Fukuzumi, S.; El Ojaimi, M.; Gros, C. P.; Barbe, J. M.; Gullard, R. *Inorg. Chem.* **2009**, *48*, 2571–2582.
(21) Gao, Y.; Akermark, T.; Liu, J. H.; Sun, L. C.; Akermark, B. *J. Am. Chem. Soc.* **2009**, *131*, 8726–8727.

scaffold bear two corroles or a corrole and a porphyrin.[23,24] Adapting Lindsey porphyrin[25] and Gryko corrole forming conditions,[26] we now report synthetic methods for: (i) a one-pot route to deliver 5,10,15-tris(pentafluorophenyl) corrole in good yields and a new class of compounds, the (ii) hangman corroles (HCX), which have been structurally characterized. We go on to show by spectroscopy, augmented by density functional theory (DFT), that the cobalt hangman corroles are capable of accessing high oxidation states in which the corrole is a noninnocent redox ligand. The PCET reactivity of the cobalt hangman corroles is demonstrated for the four-electron, four-proton reduction of oxygen, where a key intermediate for this reaction, a cobalt corrole superoxide complex, has been observed spectroscopically.

Experimental Section

General Methods. ^{1}H NMR spectra (500 MHz) were recorded on samples in $CDCl_3$ at room temperature unless noted otherwise. Silica gel (60 μm average particle size) was used for column chromatography. Compounds **4**−**7**[10] and **8**−**10**[27] were prepared as described in the literature. THF (anhydrous), methanol (anhydrous), CH_2Cl_2 (anhydrous), $CHCl_3$ and all other chemicals were reagent grade and used as received. LD-MS data were collected in the presence of a 1,4-di-(2−5-phenyl-oxazolyl)benzene matrix.

Microwave-assisted reactions (deprotection and metalation of corroles) were performed inside the cavity of a CEM Discover microwave synthesis system equipped with infrared, pressure and temperature sensors to monitor synthesis conditions. The reaction vessels were 10 mL crimp-sealed thick-wall glass tubes. The contents of each vessel were stirred with a magnetic stirrer.

General Protocol for the Synthesis of Hangman Corroles (Method A). The Gryko corrole forming reaction[26] was optimized. CH_2Cl_2 (20 mL) was placed in an oven-dried round-bottom flask (250 mL). A sample of compound **7**[10] (0.244 g, 0.600 mmol) and the corresponding dipyrromethane (1.50 mmol) were added to the reaction flask. The reaction mixture was stirred about 10 min to obtain a homogeneous mixture. In a separate flask, 1.3 mM TFA (10 μL TFA was mixed with 100 mL CH_2Cl_2) solution was prepared. A sample of freshly prepared TFA solution (20 mL) was slowly added to first flask via syringe. A septum was placed and the reaction mixture was stirred for 7 h at room temperature. A sample of 2,3-dichloro-5,6-dicyano-1,4-benzoquinone (DDQ, 0.340 g, 1.50 mmol) was added and the reaction mixture was stirred for 15 min. The reaction mixture was loaded directly on a silica gel column and eluted with dichloromethane until the first fluorescent band was collected. Further purification of the compound by flash column chromatography (silica, hexanes/ethanol (9:1)) afforded a dark violet solid.

General Protocol for Basic Hydrolysis of Hangman Corroles under Microwave Irradiation (Method B). A sample of HCX-CO_2Me (0.1 mmol) was placed in a microwave glass tube (10 mL) containing a magnetic stir bar. THF (2 mL, HPLC grade lacking stabilizer) was added. The resulting mixture was stirred to obtain a homogeneous solution. A sample of 6 N NaOH (2 mL) was added. The vessel was sealed with a septum and subjected to microwave irradiation at 75 °C. The protocol was as follows: (1) heat the reaction vessel from room temperature to 75 °C, (2) hold at 75 °C and irradiate for 10 min (temperature overshoots of 80−85 °C were permitted; temperature was re-established at 75 °C by using open flow valve option), (3) allow the reaction mixture to cool to room temperature, (4) check the reaction mixture by silica TLC analysis, and (5) repeat steps 1 − 4 until all of the HCX-CO_2Me starting material was consumed. The reaction mixture was transferred to a flask, and diluted with 100 mL of CH_2Cl_2. The organic phase was separated, washed with water, brine and concentrated. The resulting crude product was dissolved in CH_2Cl_2 (100 mL), and treated with 20% HCl (50 mL). The reaction mixture was stirred at room temperature for 8 − 12 h. The organic phase was separated, and washed with water until the solution changed from green to purple, and then the solution was washed with brine, dried over Na_2SO_4, and concentrated to dryness. The resulting crude product was chromatographed (silica, CH_2Cl_2) to afford the corresponding hangman corrole featuring the carboxylic acid hanging group.

General Protocol for Metalation of Corroles under Microwave Irradiation (Method C). A microwave glass tube (10 mL) containing a magnetic stir bar was charged with CH_3CN or $CHCl_3$ and the corrole. The solution was stirred at room temperature for 10 min to obtain a homogeneous mixture. The metal salt was added (5−10 mol equiv versus corresponding hangman corrole) and the resulting mixture was stirred at room temperature for 10 min. The reaction vessel was sealed with a septum and subjected to microwave irradiation at 65 °C, for reactions performed in $CHCl_3$ and at 85 °C for reactions performed in CH_3CN. The protocol was as follows: (1) heat the reaction vessel from room temperature to 65 °C (85 °C for CH_3CN), (2) hold at 65 °C (85 °C for CH_3CN) and irradiate for 20 min (temperature overshoots of 70−75 °C (90−95 °C for CH_3CN)) were permitted; temperature was re-established at 70 °C (85 °C for CH_3CN) by using open flow valve option), (3) allow the reaction mixture to cool to room temperature, (4) check the reaction mixture by silica TLC analysis, (5) repeat steps 1−4 until all of the free base corrole was consumed. Upon complete reaction, triethylamine (10 mol equiv to metal salt) was added to the solution, which was washed with water and brine, dried over Na_2SO_4, and concentrated to dryness. The resulting crude product was chromatographed on silica to afford the corresponding metal complex corrole.

5,10,15-Tris(pentafluorophenyl)corrole (1). By following modified Lindsey porphyrin forming reaction,[25] $CHCl_3$ (900 mL) was placed in an oven-dried round-bottom flask (1000 mL) and purged with high flow of argon for 40 min. Pyrrole (5.5 mL, 80 mmol), paraformaldehyde (0.15 g, 5.0 mmol) and pentafluorobenzaldehyde (9.2 mL, 75 mmol) were added to the reaction flask, which was covered with aluminum foil. The solution was purged with argon for 45 min. A sample of $BF_3 \cdot OEt_2$ (3.3 mL, 26 mmol) was added to the reaction mixture dropwise via syringe and the solution stirred under argon in the dark for 45 min. DDQ (4.5 g, 20 mmol) was added, and the resulting mixture was stirred for an additional 1 h. A sample of triethylamine (3.6 mL, 26 mmol) was added and the reaction mixture was stirred for additional 20 min. The resulting reaction mixture was concentrated to dryness and the crude product was subjected to silica chromatography (hexanes → hexanes:CH_2Cl_2 (6:1) → hexanes:CH_2Cl_2 (4:1)) to afford a purple solid (1.342 g, 7% based on pentafluorobenzaldehyde). ^{1}H NMR, ESI-MS and absorption spectral data are consistent with that reported in the literature.[28]^{1}H NMR (500 MHz, $CDCl_3$) δ/ppm: 8.52−8.63 (broad s, 2H), 8.68 (d, J = 4.5 Hz, 2H), 8.85 (d, J = 4.5 Hz, 2H), 9.03 (d, J = 4.5 Hz, 2H), pyrrolic (3H) were not observed at room temperature. HR(ESI)-MS (M+H) ($M = C_{37}H_{11}F_{15}N_4$): Calcd for m/z = 797.0817, obsd 797.0834. LD-MS obsd 796.11; $\lambda_{max,abs}$ /nm (CH_2Cl_2) = 416, 561, 604. $\lambda_{max,em}$(416 exc) /nm = 643. Anal. calcd

(22) Paolesse, R. In *The Porphrin Handbook*; Kadish, K. M., Smith, K. M., Guilard, R., Eds.; Academic Press: New York, 2000; Vol. 2, Chapter 12.
(23) Guilard, R.; Jerome, F.; Barbe, J.-M.; Gros, C. P.; Ou, Z.; Shao, J.; Fischer, J.; Weiss, R.; Kadish, K. M. *Inorg. Chem.* **2001**, *40*, 4856–4865.
(24) Kadish, K. M.; Ou, Z.; Shao, J.; Gros, C. P.; Barbe, J.-M.; Jerome, F.; Bolze, F.; Burdet, F.; Guilard, R. *Inorg. Chem.* **2002**, *41*, 3990–4005.
(25) Lindsey, J. S.; Wagner, R. W. *J. Org. Chem.* **1989**, *54*, 828–836.
(26) Gryko, D. T.; Jadach, K. *J. Org. Chem.* **2001**, *66*, 4267–4375.
(27) Laha, J. K.; Dhanalekshmi, S.; Taniguchi, M.; Ambroise, A.; Lindsey, J. S. *Org. Process Res. Dev.* **2003**, *7*, 799–812.
(28) Gross, Z.; Galili, N.; Saltsman, I. *Angew. Chem.* **1999**, *38*, 1427–1429.

for $C_{37}H_{11}F_{15}N_4$: C, 55.79; H, 1.39; N, 7.03. Found: C, 55.30; H, 0.96; N, 6.95.

5,10,15-Tris(pentafluorophenylcorrolato)cobalt(III) (1-Co). Method C was followed. A solution of **1** (79 mg, 0.099 mmol) in CH_3CN (2 mL) was treated with $Co(OAc)_2$ (175 mg, 0.990 mmol). The standard workup was followed by column chromatography (silica, Hexanes/CH_2Cl_2 (1:1) → CH_2Cl_2) to afford a dark-brown solid (79 mg, 95%). ^{1}H NMR (500 MHz, $CDCl_3$) δ/ppm: 6.48 (d, J = 4.5 Hz, 2H), 6.53 (d, J = 4.5 Hz, 2H), 6.78−6.86 (m, 2H), 7.08−7.14 (m, 2H). HR(ESI)-MS in negative ion mode (M^-) (M = $C_{37}H_8F_{15}N_4Co$): Calcd for m/z = 851.9847, obsd 851.9835. LD-MS obsd 852.42, dimer 1073.68, trimer 2554.04; $\lambda_{max,abs}$ /nm (CH_2Cl_2) = 398, 534. Anal. calcd for $C_{37}H_8F_{15}N_4Co$: C, 52.13; H, 0.95; N, 6.57. Found: C, 52.16; H, 1.09; N, 7.07.

10-(4-(5-Methoxycarbonyl-2,7-ditert-butyl-9,9-dimethylxanthene))-5,15-bis(pentafluorophenyl)corrole (HCX1-CO_2Me). Method A was followed. A mixture of **7** (0.244 g, 0.600 mmol) and 5-pentafluorophenyl dipyrromethane **8** (0.468 g, 1.50 mmol) in CH_2Cl_2 (20 mL) were treated with 1.3 M freshly prepared TFA solution (20 mL). The reaction mixture was stirred for 7 h and treated with DDQ (0.340 g, 1.50 mmol). The resulting crude product was chromatographed to afford a purple solid (139 mg, 23%). ^{1}H NMR (500 MHz, $CDCl_3$) δ/ppm: 1.03 (s, 3H), 1.27 (s, 9H), 1.50 (s, 9H), 1.91 (s, 6H), 7.29 (d, J = 2.5 Hz, 1H), 7.65 (d, J = 2.5 Hz, 1H), 7.85 (d, J = 2.5 Hz, 1H), 7.91 (d, J = 2.5 Hz, 1H), 8.52−8.56 (m, 2H), 8.65 (s, 4H), 9.12 (d, J = 4.5 Hz, 2H), pyrrolic protons were not observed at room temperature. HR(ESI)-MS (M + H) (M = $C_{56}H_{42}F_{10}N_4O_3$): Calcd for m/z = 1009.3170, obsd 1009.3153. LD-MS obsd 1009.17. $\lambda_{max,abs}$/nm (CH_2Cl_2) = 411, 558, 613. $\lambda_{max,em}$(414 exc)/nm = 648. Anal. calcd for $C_{56}H_{42}F_{10}N_4O_3 \cdot 2H_2O$: C, 64.37; H, 4.44; N, 5.36. Found: C, 64.24; H, 4.07; N, 5.61.

10-(4-(5-Methoxycarbonyl-2,7-ditert-butyl-9,9-dimethylxanthene))-5,15-bis(pentafluorophenyl)cobaltcorrole (CoHXC1-CO_2Me). Method C was followed. A solution of **HCX1-CO_2Me** (100 mg, 0.10 mmol) in CH_3CN (2 mL) was treated with $Co(OAc)_2$ (88 mg, 0.50 mmol). Standard workup was followed by column chromatography (silica, $CHCl_3$ → $CHCl_3$:MeOH (100:1) → $CHCl_3$:MeOH (10:1)) to afford a dark brown solid (82 mg, 78%). HR(ESI)-MS (M^-) (M = $C_{56}H_{39}CoF_{10}N_4O_3$): Calcd for m/z = 1064.2200, obsd 1064.2242. LD-MS obsd 1064.55. $\lambda_{max,abs}$/nm (CH_2Cl_2) = 310, 425, 620. Anal. calcd for $C_{56}H_{39}CoF_{10}N_4O_3$: C, 63.16; H, 3.69; N, 5.26. Found: C, 62.96; H, 3.78; N, 5.22.

10-(4-(5-Hydroxycarbonyl-2,7-ditert-butyl-9,9-dimethylxanthene))-5,15-bis(pentafluorophenyl)corrole (HCX1-CO_2H). Method B was followed. A solution of **HCX1-CO_2Me** (100 mg, 0.0992 mmol) in THF (1 mL) was treated with 6 N NaOH (2 mL). The reaction mixture was subjected to microwave irradiation for 6 h. The aqueous work up was performed and the resulting crude was treated with 20% HCl. The biphasic reaction mixture was stirred overnight. The organic phase was separated, and washed. The crude product was chromatographed (silica, hexanes/CH_2Cl_2 (5:3) → hexanes/CH_2Cl_2 (5:2) → CH_2Cl_2) to afford a purple solid (81 mg, 82%). ^{1}H NMR (500 MHz, $CDCl_3$) δ/ppm: 1.27 (s, 9H), 1.54 (s, 9H), 1.97 (s, 6H), 7.60−7.62 (m, 1H), 7.77−7.78 (m, 1H), 7.96−7.97 (m, 1H), 8.0−8.04 (m, 1H), 8.65−8.68 (m, 4H), 8.75−8.76 (m, 2H), 9.21 (d, J = 4.0 Hz, 2H), pyrrolic (3H) and carboxylic acid protons were not observed at room temperature. HR(ESI)-MS (M − H) (M = $C_{55}H_{40}F_{10}N_4O_3$): Calcd for m/z = 993.2868, obsd 993.2859. LD-MS obsd 994.3. $\lambda_{max,abs}$/nm (CH_2Cl_2) = 409, 563, 610. $\lambda_{max,em}$(409 exc) /nm = 651.

10-(4-(5-Hydroxycarbonyl-2,7-ditert-butyl-9,9-dimethylxanthene))-5,15-bis(pentafluorophenyl)cobaltcorrole (CoHCX1-CO_2H). Method C was followed. A solution of **HCX1-CO_2H** (93 mg, 0.10 mmol) in CH_3CN (2 mL) was treated with $Co(OAc)_2$ (88 mg, 0.50 mmol). Standard workup was followed by column chromatography (silica, $CHCl_3$ → $CHCl_3$:MeOH (100:1) → $CHCl_3$:MeOH (10:1)) to afford a dark brown solid (72 mg, 69%). HR(ESI)-MS (M + H) (M = $C_{55}H_{37}CoF_{10}N_4O_3$): Calcd for m/z = 1050.2043, obsd 1050.2143. LD-MS obsd 1050.78. $\lambda_{max,abs}$/nm (CH_2Cl_2) = 303, 430, 609. Anal. calcd for $C_{55}H_{37}CoF_{10}N_4O_3 \cdot 3H_2O$: C, 59.79; H, 3.92; N, 5.07. Found: C, 59.77; H, 4.09; N, 5.26.

10-(4-(5-Methoxycarbonyl-2,7-ditert-butyl-9,9-dimethylxanthene))-5,15-bis(4-tert-butylphenyl)corrole (HCX2-CO_2Me). Method A was followed. A mixture of **7** (0.244 g, 0.600 mmol), and 5-*tert*-butyl dipyrromethane **9** (0.418 g, 1.50 mmol) in CH_2Cl_2 (20 mL) was treated with 1.3 M freshly prepared TFA solution (20 mL). The reaction mixture was stirred for 7 h and treated with DDQ (0.340 g, 1.50 mmol). The resulting crude product was chromatographed to afford a purple solid (113 mg, 20%). ^{1}H NMR (500 MHz, $CDCl_3$) δ/ppm: 0.85 (s, 3H), 1.29 (s, 9H), 1.50 (s, 9H), 1.59 (s, 18H), 1.91 (s, 6H), 7.34 (d, J = 2.5 Hz, 1H), 7.65 (d, J = 2.5 Hz, 1H), 7.81 (d, J = 2.5 Hz, 1H), 7.84 (d, J = 4.5 Hz, 4H), 7.94 (d, J = 2.5 Hz, 1H), 8.32−8.34 (m, 4H), 8.48 (d, J = 4.5 Hz, 2H), 8.62 −8.64 (m, 2H), 8.89 (d, J = 4.5 Hz, 2H), 8.94−8.96 (m, 2H). The pyrrolic protons (3H) were not observed at room temperature; HR(ESI)-MS (M + H) (M = $C_{64}H_{68}N_4O_3$): Calcd for m/z = 941.5364, obsd 941.5368 LD-MS obsd 940.8. $\lambda_{max,abs}$/nm (CH_2Cl_2) = 407, 425, 559, 602, 634. $\lambda_{max,em}$(407 exc) /nm = 642. Anal. calcd for $C_{64}H_{68}N_4O_3$: C, 81.67; H, 7.28; N, 5.95. Found: C, 81.72; H, 7.51; N, 5.67.

10-(4-(5-Hydroxycarbonyl-2,7-ditert-butyl-9,9-dimethylxanthene))-5,15-bis(4-tert-butylphenyl)corrole (HCX2-CO_2H). Method B was followed. A solution of **HCX2-CO_2Me** (94 mg, 0.10 mmol) in THF (1 mL) was treated with 6 N NaOH (2 mL). The reaction mixture was subjected to microwave irradiation for 8 h. The aqueous work up was performed and the resulting crude was treated with 20% HCl. The biphasic reaction mixture was stirred overnight. The organic phase was separated, and washed. The crude product was chromatographed (silica, CH_2Cl_2) to afford a purple solid (65 mg, 70%). ^{1}H NMR (500 MHz, $CDCl_3$) δ/ppm: 1.28 (s, 9H), 1.53 (s, 9H), 1.59 (s, 18H), 1.98 (s, 6H), 7.73 (s, 1H), 7.76 (s, 1H), 7.80−7.83 (m, 4H), 7.88 (s, 1H), 8.02 (s, 1H), 8.30−8.32 (m, 4H), 8.42−8.45 (m, 2H), 8.62−8.65 (m, 2H), 8.90−8.02 (m, 2H), 8.97−8.99 (m, 2H). The pyrrolic (3H) and carboxylic acid protons were not observed at room temperature. HR(ESI)-MS (M + H) (M = $C_{63}H_{66}N_4O_3$): Calcd for m/z = 927.5313, obsd 927.5211. LD-MS obsd 926.55. $\lambda_{max,abs}$/nm (CH_2Cl_2) = 407, 426, 565, 600, 634. $\lambda_{max,em}$(407 exc) /nm = 645. Anal. calcd for $C_{63}H_{66}N_4O_3$: C, 81.61; H, 7.17; N, 6.04. Found: C, 81.20; H, 6.90; N, 5.97.

10-(4-(5-Hydroxycarbonyl-2,7-ditert-butyl-9,9-dimethylxanthene))-5,15-bis(4-tert-butylphenyl)cobaltcorrole (CoHCX2-CO_2H). Method C was followed. A solution of **HCX2-CO_2H** (92 mg, 0.10 mmol) in CH_3CN (2 mL) was treated with $Co(OAc)_2$ (88 mg, 0.50 mmol). Standard workup was followed by column chromatography (silica, $CHCl_3$ → $CHCl_3$: MeOH (100:1) → $CHCl_3$:MeOH (10:1)) to afford a dark brown solid (83 mg, 89%). HR(ESI)-MS (M + H) (M = $C_{63}H_{63}CoN_4O_3$): Calcd for m/z = 982.4232, obsd 982.4225. LD-MS obsd 982.02, dimer 1964.59. $\lambda_{max,abs}$/nm (CH_2Cl_2) = 358, 438, 529. Anal. calcd for $C_{63}H_{63}CoN_4O_3 \cdot 3H_2O$. C, 72.96; H, 6.71; N, 5.40. Found: C, 73.34; H, 6.14; N, 5.77.

10-(4-(5-Methoxycarbonyl-2,7-ditert-butyl-9,9-dimethylxanthene))-5,15-bis(2,4,6-trimethylphenyl)corrole (HCX3-CO_2Me). Method A was followed. A mixture of **7** (0.244 g, 0.600 mmol), and 5-mesityl dipyrromethane **10** (0.396 g, 1.50 mmol) in CH_2Cl_2 (20 mL) was treated with 1.3 M freshly prepared TFA solution (20 mL). The reaction mixture was stirred for 7 h and treated with DDQ (0.340 g, 1.50 mmol). The resulting crude product was chromatographed to afford a purple solid (107 mg, 19%). ^{1}H NMR (500 MHz, $CDCl_3$) δ/ppm: 0.55 (s, 3H), 1.26 (s, 9H), 1.47 (s, 9H), 1.87 (s, 6H), 1.89 (s, 6H), 2.04 (s, 6H), 2.59 (s, 6H), 7.22−7.28 (m, 2H), 7.26−7.27 (m, 2H, overlapped with $CDCl_3$ peak), 7.33 (d, J = 2.5 Hz, 1H), 7.64 (d, J = 2.5 Hz, 1H), 7.78 (d, J = 2.5 Hz, 1H), 7.86 (d, J = 2.5 Hz, 1H), 8.32 (d, J = 4 Hz, 2H), 8.39 (d, J = 4.5 Hz, 2H), 8.43 (d, J = 4.5 Hz, 2H), 8.88 (d, J = 4 Hz, 2H). The pyrrolic protons (3H) were not observed at room temperature. HR(ESI)-MS (M + H) (M = $C_{62}H_{64}N_4O_3$): Calcd for m/z = 913.5051, obsd 913.5033. LD-MS obsd 912.62. $\lambda_{max,abs}$ /nm (CH_2Cl_2) = 406, 423,

559, 601, 633. $\lambda_{max,em}$(414 exc) /nm = 645. Anal. calcd for $C_{63}H_{66}N_4O_3$: C, 81.54; H, 7.06; N, 6.14. Found: C, 81.59; H, 6.94; N, 6.18.

10-(4-(5-Hydroxycarbonyl-2,7-ditert-butyl-9,9-dimethylxanthene))-5,15-bis(2,4,6-trimethylphenyl)corrole (HCX3-CO_2H). Method B was followed. A solution of **HCX3-CO_2Me** (92 mg, 0.10 mmol) in THF (1 mL) was treated with 6 N NaOH (2 mL). The reaction mixture was subjected to microwave irradiation for 8 h. The aqueous work up was performed and the resulting crude was treated with 20% HCl. The biphasic reaction mixture was stirred overnight. The organic phase was separated, and washed. Silica chromatography (CH_2Cl_2) afforded a purple solid (63 mg, 70%). ^{1}H NMR (500 MHz, $CDCl_3$) δ/ppm: 1.26 (s, 9H), 1.52 (s, 9H), 1.87 (s, 6H), 1.94 (s, 6H), 2.03 (s, 6H), 2.59 (s, 6H), 7.23−7.24 (m, 2H), 7.26−7.27 (m, 2H, overlapped with $CDCl_3$ peak), 7.69 (d, J = 2.5 Hz, 1H), 7.72 (d, J = 2.0 Hz, 1H), 7.85 (d, J = 2.0 Hz, 1H), 8.05 (d, J = 2.0 Hz, 1H), 8.33 (d, J = 4 Hz, 2H), 8.37 (d, J = 4.5 Hz, 2H), 8.46 (d, J = 4.5 Hz, 2H), 8.91 (d, J = 4 Hz, 2H). The pyrrolic (3H) and carboxylic acid protons were not observed at room temperature. HR(ESI)-MS (M + H) (M = $C_{61}H_{62}N_4O_3$): Calcd for m/z = 899.4895, obsd 899.4888. $\lambda_{max,abs}$/nm (CH_2Cl_2) = 408, 425, 566, 601, 635, $\lambda_{max,em}$(408 exc) /nm = 648. Anal. calcd for $C_{61}H_{62}N_4O_3$: C, 81.48; H, 6.95; N, 6.23. Found: C, 80.95; H, 6.49; N, 6.05.

10-(4-(5-Hydroxycarbonyl-2,7-ditert-butyl-9,9-dimethylxanthene))-5,15-bis(2,4,6-trimethylphenyl)cobaltcorrole (CoHCX3-CO_2H). Method C was followed. A solution of **HCX3-CO_2H** (95 mg, 0.11 mmol) in CH_3CN (2 mL) was treated with $Co(OAc)_2$ (88 mg, 0.50 mmol). Standard workup was followed by column chromatography (silica,$CHCl_3$ → $CHCl_3$: MeOH (100:1) → $CHCl_3$:MeOH (10:1)) to afford a dark brown solid (78 mg, 81%). HR(ESI)-MS (M − H) (M = $C_{61}H_{59}CoN_4O_3$): Calcd for m/z = 953.3846 obsd 953.3839. LD-MS obsd 954.63. $\lambda_{max,abs}$ /nm (CH_2Cl_2) = 404, 534. Anal. calcd for $C_{61}H_{59}C_ON_4O_3$. C, 76.71; H, 6.23; N, 5.87. Found: C, 76.39; H, 6.25; N, 5.27.

X-Ray Crystallographic Details. Single crystals of **1-CoCl**, **HCX1-CO_2H** and **HCX2-CO_2Me** were obtained by slow evaporation of a hexanes and CH_2Cl_2 mixture. **1-CoCl** was mounted on a Bruker three circle goniometer platform equipped with an APEX detector. A single crystal of **HCX2-CO_2Me** was mounted on a Bruker three circle goniometer platform equipped with an APEX 2 detector, whereas **HCX1-CO_2H** was mounted on a Bruker four circle goniometer equipped with an APEX 2 detector. A graphite monochromator was employed for wavelength selection of the Cu Kα radiation (λ = 1.54178 Å, **HCX2-CO_2Me** and **HCX1-CO_2H**) or Mo Kα radiation (λ = 0.71073 Å, **1-CoCl**). The data were processed and refined using the program SAINT supplied by Siemens Industrial Automation. Structures were solved by direct methods in SHELXS and refined by standard difference Fourier techniques in the SHELXTL program suite (6.10 v., Sheldrick G. M., and Siemens Industrial Automation, 2000). For the solution of the **1-CoCl** structure, hydrogen atoms were placed in calculated positions using the standard riding model and refined isotropically; all other atoms were refined anisotropically. For the solution of the **HCX2-CO_2Me** and **HCX1-CO_2H** structures, hydrogen atoms bound to nitrogen or oxygen were located in the difference map and restrained to a distance of 0.84 (O−H) or 0.88 (N−H) Å. The isotropic displacement parameters of the hydrogen atoms were fixed to 1.2 times the U value of the atoms to which they are bonded. All non-hydrogen atoms were refined anisotropically. The structure of **1-CoCl** contained a dichloromethane solvate molecule that was modeled as a two-part disorder. The structure of **HCX1-CO_2H** contained a disordered hexane molecule modeled in a similar fashion. The (1,2) and (1,3) distances of all disordered parts were restrained to be similar using the SADI command; the rigid-bond restraints SIMU and DELU were also used on disordered parts. In the disordered hexane of molecule of **HCX1-CO_2H**, distance restraints were used to fix carbon−carbon 1−2 and 1−3 distances (1.54 Å and 2.52 Å, respectively). Unit cell parameters, morphology, and solution statistics are summarized in Table S1 (Supporting Information). All thermal ellipsoid plots are drawn at 50% probability level, with solvent molecules omitted.

Cyclic Voltammetry. Cyclic voltammograms (CV) were recorded in CH_3CN or CH_2Cl_2 solutions containing 0.1 M NBu_4PF_6 (tetrabutylammonium hexafluorophosphate) and the corrole compound at 1.05 mM. A three compartment cell was employed possessing a 0.07 cm^2 glassy carbon button electrode as the working electrode, Pt wire as the auxiliary electrode, and Ag/AgCl as a reference electrode. CVs were collected with scan rates of 10−100 mV/s with *iR* compensation.

Spectroscopic Methods. UV−vis spectra were recorded on a Varian Cary 5000 UV−vis-NIR spectrophotometer on solutions of anhydrous CH_2Cl_2, THF or CH_2Cl_2:EtOH (3:1) at room temperature contained in quartz cuvettes. Steady state emission spectra were recorded on an automated Photon Technology International (PTI) QM 4 fluorimeter equipped with a 150-W Xe arc lamp and a Hamamatsu R928 photomultiplier tube. Excitation light was wavelength selected with glass filters. Solution samples were prepared under ambient atmosphere in anhydrous CH_2Cl_2 or THF and contained in screw-cap quartz fluorescence cells.

Continuous wave X-band EPR spectra were recorded using a Bruker ESP 300 spectrometer, fitted with an Oxford ESR 910 cryostat cooled with liquid helium. All spectra were recorded on frozen solution samples at temperatures of 2−80 K. Data analysis and spectral simulations were executed using the SpinCount software package developed by Prof. Mike Hendrich at Carnegie Mellon University.[29] EPR spectra of the oxygen adduct were simulated akin to the analysis of the EPR spectra recorded for single crystals of the oxygen adduct of vitamin B12.[30,31] As such, in order to get a good representation of the experimental data we found that the A^{Co} tensor, $A_1 = 91 \pm 8$ MHz, $A_2 = 29 \pm 4$ MHz, and $A_3 = 35 \pm 2$ MHz, needs to be rotated from the g-tensor, $g_1 = 2.11 \pm 0.01$, $g_2 = 2.02 \pm 0.01$, $g_3 = 1.98 \pm 0.01$ by $\alpha = 12° \pm 5°$ and $\beta = 9° \pm 5°$.

The DFT calculations were performed with Gaussian'09 (revision A.2.) quantum mechanical software package. The B3LYP/6-311G hybrid functional/basis set combination was used for all calculations. For **1-CoCl**, a structural geometric model with an initial C_s point group symmetry was constructed and used as starting point for geometry optimization. Subsequent optimizations by relieving the symmetry constraints did not lead to a distortion from the stationary point found for the C_s point group. The nature of the predicted electronic state was assessed on the basis of time-dependent (TD) DFT calculations, by analyzing the gross orbital population and inspecting the calculated Mulliken charges, spin densities, and values of the Fermi and spin-dipolar components of the hyperfine coupling tensors.

Oxygen Reduction Measurements. A solution was prepared consisting of 3.9 mL THF containing, 0.3 mM catalyst, 4 mg MWCNT, and 45 μL 5% Nafion. For each experiment, the mixture was sonicated for 20 min and then a 10 μL drop was applied to the surface of a polished glassy carbon electrode and allowed to evaporate to afford a film containing a MWCNT loading of 50 μg_c/cm^2 and a catalyst loading of 3 nmol. The electrocatalytic activity was measured in a 3-electrode cell in 0.5 M H_2SO_4 by rotating ring disk electrode (RRDE) techniques. For oxygen reduction, the counter electrode was a platinum wire and the reference electrode was a saturated calomel electrode calibrated against reversible hydrogen. All potentials in aqueous solution are given vs RHE. In the RRDE experiments the platinum ring was held at 1.2 V vs SCE

(29) This program can be downloaded from http://www.chem.cmu.edu/groups/hendrich/ facilities/index.html.
(30) Ramdhanie, B.; Telser, J.; Caneschi, A.; Zakharov, L. N.; Rheingold, A. L.; Goldberg, D. P. *J. Am. Chem. Soc.* **2004**, *126*, 2515–2525.
(31) Jörin, E.; Schweiger, A.; Günthard, Hs. H. *Chem. Phys. Lett.* **1979**, *61*, 228–232.

Scheme 1

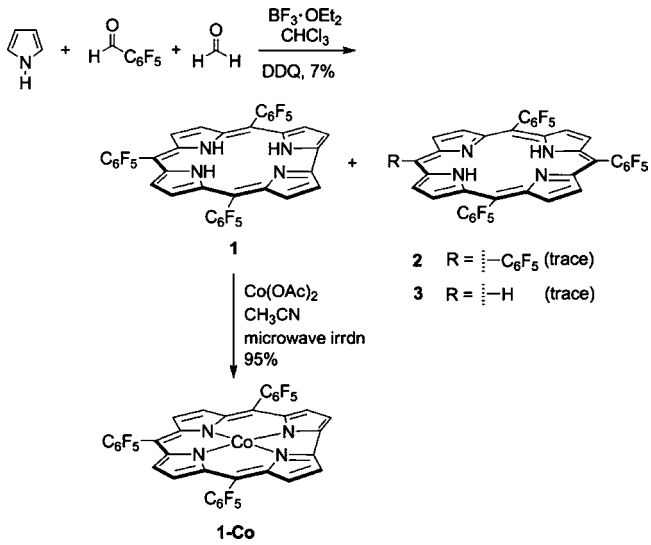

and the collection efficiency calibrated against the $Fe(CN)_6^{3-/4-}$ reduction process.[32]

Results and Discussion

Synthesis. The observation of corrole as a minor side-product with Lindsey porphyrin synthesis conditions prompted us to investigate the reaction conditions in detail with the goal of obtaining A_3 corrole monomer as a major product. The synthesis of the 5,10,15-tris(pentafluorophenyl)corrole (**1**) was undertaken as an exemplar; the synthetic strategy is shown in Scheme 1. Large scale (75 mmol) synthesis of **1** was performed by condensation of commercially available pyrrole, pentafluorobenzaldehyde and paraformaldehyde under Lindsey conditions.[25] Paraformaldehyde has been utilized for the syntheses of corrole monomer and corrole dimer.[33] The role of paraformaldehyde in the corrole forming reaction, though not delineated, is likely to tune the acid concentration for the formation of a bilane that delivers corrole rather than corresponding porphyrin. What is certain is that if paraformaldehyde is not used, the formation of porphyrin is preferred. Thin layer chromatography (TLC) and matrix-assisted laser desorption/ionization time of flight (MALDI-TOF) analysis of the crude reaction mixture revealed **1** as a major product. Trace amounts of porphyrins **2** and **3** were also observed as side products. The desired product **1** was isolated by flash column chromatography in 7% yield. We note that the yield of the corrole diminishes when the reaction is executed on small scale (3.75 mmol) and A_4 porphyrin **2** is obtained in greater predominance.

The new synthesis of tris(pentafluorophenyl)corrole, **1**, is an advance over previous methods for the following reasons. (1) The new route affording compound **1** does not require harsh conditions (room temperature vs 100 °C) for intramolecular cyclization. The corrole forming reaction at higher cyclization temperature causes partial decomposition of the bilane intermediate and the polymerization of the linear tetrapyrrolic species which reduces the yield for corrole formation dramatically. (2) The corrole forming reaction at lower concentration favors the desired intramolecular cyclization of the bilane as opposed to intermolecular reaction between dipyrromethane species at the higher concentrations of previous methods. The former reaction

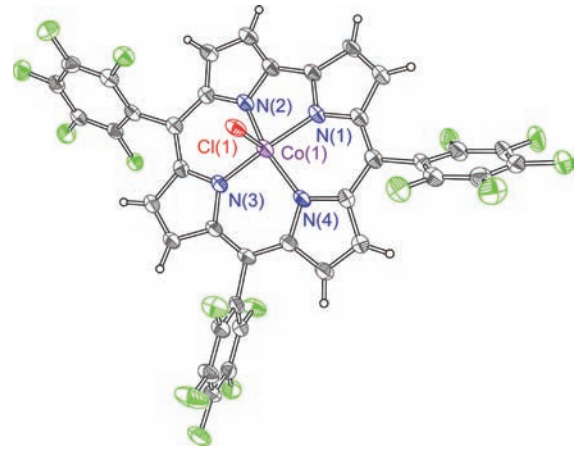

Figure 1. Crystal structure of **1-CoCl** with ellipsoids shown at the 50% probability level. The dichloromethane solvate is omitted for clarity, and H-atoms are shown in idealized positions. Data were collected at 100(2) K.

affords formation of the corresponding porphyrin instead of target corrole. (3) The route described here does not require presence of solid support such as, florisil, silica or alumina for corrole synthesis. Finally, (4) the synthesis is scalable and affords the corrole in a one-pot synthesis at much higher yields.

Microwave irradiation has been employed for the synthesis of free base corrole monomers[34] and for the metalation of porphyrin,[35] though a similar metalation chemistry for corroles has yet to be explored. We find that microwave irradiation of corroles in the presence of a metal acetate drives metalation in high yields; microwave irradiation of **1** in the presence of excess $Co(OAc)_2$ affords **1-Co** in 95% isolated yield. On the basis of the ^1H NMR spectrum and SQUID data, **1-Co** is paramagnetic. The magnetic moment is ca. 1 cm^3K/mol at room temperature, which decreases gradually to 0.1 cm^3K/mol at 2 K.

Crystals of **1-CoCl** were obtained by slow evaporation of a dichloromethane solution of **1-Co**; the source of Cl is likely from trace impurities of HCl in the dichloromethane. The X-ray crystal structure of **1-CoCl** is shown in Figure 1; the central cobalt atom resides in a square pyramidal coordination environment and the corrole macrocycle shows only slight deviations from an ideal planar system. The Co−N distances are not equally distributed; they are split into two groups. The Co−N bonds on the side with the direct C−C pyrrole bridge are shorter (1.888 and 1.887 Å) than those opposite to the methylene pyrrole bridge (1.911 and 1.923 Å). One of the pentafluorophenyl substituents is almost perpendicular to the macrocycle plane (83°) whereas the other two are considerably less twisted (~59°). The Co−Cl distance is 2.243 Å and the displacement of the cobalt atom out of the N_4-plane is 0.413 Å. This displacement is unusually large relative to that of known five-coordinate Co(III) corroles, which exhibit displacements between 0.29 and 0.38 Å from the plane.[36−40] These results contrast six coordinate

(32) Myuller, L.; Nekrasov, L. *Electrochim. Acta* **1964**, *9*, 1015–1023.
(33) Koszarna, B.; Gryko, D. T. *Chem. Commun.* **2007**, 2994–2996.
(34) Collman, J. P.; Decreau, R. A. *Tetrahedron Lett.* **2003**, *44*, 1207–1210.
(35) Liu, M. O.; Hu, A. T. *J. Organomet. Chem.* **2004**, *689*, 2450–2455.
(36) Hitchcock, P. B.; McLaughlin, G. M. *J. Chem. Soc., Dalton Trans.* **1976**, 1927–1930.
(37) Paolesse, R.; Licoccia, S.; Bandoli, G.; Dolmella, A.; Boschi, T. *Inorg. Chem.* **1994**, *33*, 1171–1176.
(38) Will, S.; Lex, J.; Vogel, E.; Adamian, V. A.; Vancaemelbecke, E.; Kadish, K. M. *Inorg. Chem.* **1996**, *35*, 5577–5583.
(39) Barbe, J. M.; Burdet, F.; Espinosa, E.; Guilard, R. *Eur. J. Inorg. Chem.* **2005**, *6*, 1032–1041.

Scheme 2[a]

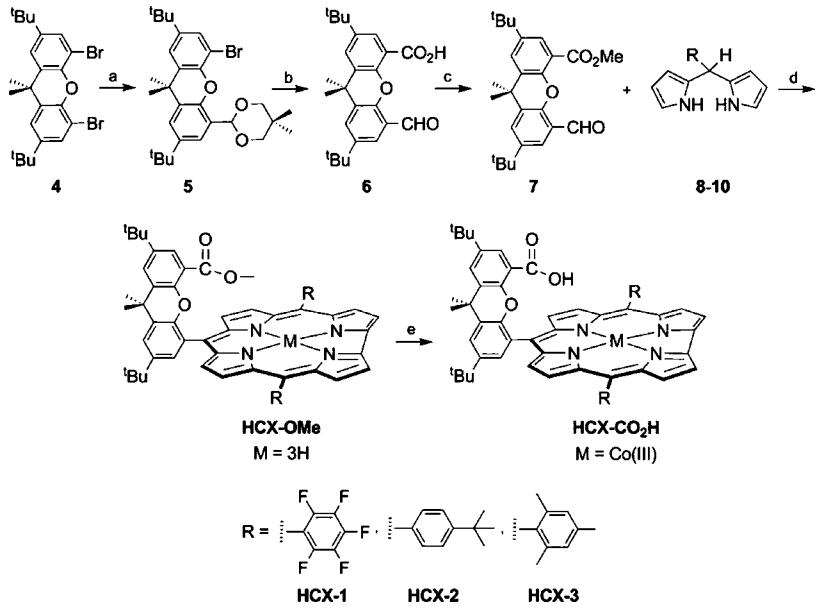

[a] (a) (1) Phenyllithium in Hexanes-THF; (2) DMF, H_2O; (3) neopentyl glycol, *p*-toluenesulfonic acid, toluene, under Ar, reflux. (b) (1) Phenyllithium in hexanes-THF; (2) CO_2(g), (3) trifluoroacetic acid, water. (c) Methanol, H_2SO_4, reflux. (d) (1) DPM **8** (**HCX-1**), **9 (HCX-2)** and **10 (HCX-3)**, TFA, CH_2Cl_2; (2) DDQ. (e) (1) THF/6 N NaOH, microwave irradiation; (2) 20% HCl, (3) $Co(OAc)_2$, CH_3CN, microwave irradiation.

Co(III) corroles such as pyridine-coordinated, (Me_4Ph_5Cor)-$Co(py)_2$,[41] which displays a cobalt ion that resides within the plane of the corrole macrocycle. Similarly, a structurally characterized five-coordinate triphenylsilylacetylide-ligated cobalt(III) corrolazine displays a nearly planar geometry,[30] in stark contrast to the structure of **1-Co**. Structurally characterized Co(IV) corroles are rare, especially when axially coordinated by Cl. To the best of our knowledge, the only other example of a structurally characterized Co(IV) chloride corrole is a Pacman structure[42] bearing no aryl meso substituents. Here too the displacement of Co from the corrole plane is small (0.19 Å) relative to that observed in **1-CoCl**, though the Co−Cl distance is similar (d(Co−Cl) = 2.275(2) Å. The structural metrics for **1-CoCl** are quite similar to Fe(IV) chloride corrole complexes.[43,44]

The HCX compounds are delivered by following the procedure outlined in Scheme 2. Compounds **4**−**7** were prepared by following a published procedure.[45] Hangman corroles were obtained by modifying the conditions of Gryko for corrole formation.[26] Dipyrromethane was condensed with **7** under Brønsted acid catalyzed conditions. Our investigations establish that the macrocycle formation occurs with better yields (∼20%) when the acid conditions are 0.6 mM TFA in CH_2Cl_2 (Table 1). The presumed intermediate, bilane,[46,47] was oxidized in situ by $4e^-$ and $4H^+$ using DDQ. A crystal structure was obtained for free base **HCX2-OMe** and it is displayed in Figure 2a. The xanthene backbone is tilted considerably relative to the corrole macrocycle, with an observed angle of 69° between the mean N_4 plane and the plane defined by the six-member aryl ring of the xanthene bonded directly to the meso carbon. The macrocycle is puckered, with one of the pyrrolic nitrogens canted out of the plane defined by the three remaining pyrrole nitrogens. The three protons were found to be delocalized among all four nitrogen atoms.

Table 1. Statistical Synthesis of Hangman Corroles Xanthene under Microwave Irradiation

Corrole	R^1	Yield[a] (%)	Corrole	Yield[b](%)
HCX1-CO_2Me		23	HXC1-CO_2H	18
HCX2-CO_2Me	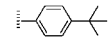	20	HCX2-CO_2H	14
HCX3-CO_2Me		19	HCX3-CO_2H	13

[a] Corrole formation was performed under Gryko conditions (ref 26). The yields are based on aldehyde **7**. [b] Overall yield is for free-base corroles, steps d and e in Scheme 2.

Deprotection of the ester functionality on the xanthene backbone is a difficult step. For hangman porphyrins, ester deprotection has been attempted under both basic and acidic conditions. The basic hydrolysis required refluxing the porphyrin

(40) Paolesse, R.; Nardis, S.; Sagone, F.; Khoury, R. G. *J. Org. Chem.* **2001**, *66*, 550–556.
(41) Guilard, R.; Gros, C. P.; Bolze, F. F.; Jerome, Z. P.; Ou, J. G.; Shao, J.; Fischer, J.; Weiss, R.; Kadish, K. M. *Inorg. Chem.* **2001**, *40*, 4845–4855.
(42) Guilard, R.; Burde, F.; Barbe, J. M.; Gros, C. P.; Espinosa, E.; Shao, J. G.; Ou, Z. P.; Zhan, R. Q.; Kadish, K. M. *Inorg. Chem.* **2005**, *44*, 3972–3983.
(43) Nardis, S.; Paolesse, R.; Licoccia, S.; Fronczek, F. R.; Vicente, M. G. H.; Shokhireva, T. K.; Cai, S.; Walker, F. A. *Inorg. Chem.* **2005**, *44*, 7030–7046.
(44) Vogel, E.; Will, S.; Tilling, A. S.; Neumann, L.; Lex, J.; Bill, E.; Trautwein, A. X.; Wieghardt, K. *Angew. Chem., Int. Ed. Engl.* **1994**, *33*, 731–735.
(45) Chng, L. L.; Chang, C. J.; Nocera, D. G. *Org. Lett.* **2003**, *5*, 2421–2424.
(46) Gossauer, A.; Engel, J. In *The Porphyrins*; Dolphin, D., Ed.; Academic Press: New York, 1978; Vol. 2, pp 197−253.
(47) Falk, H. *The Chemistry of Linear Oligopyrroles and Bile Pigments*; Springer-Verlag: Wien, 1989.

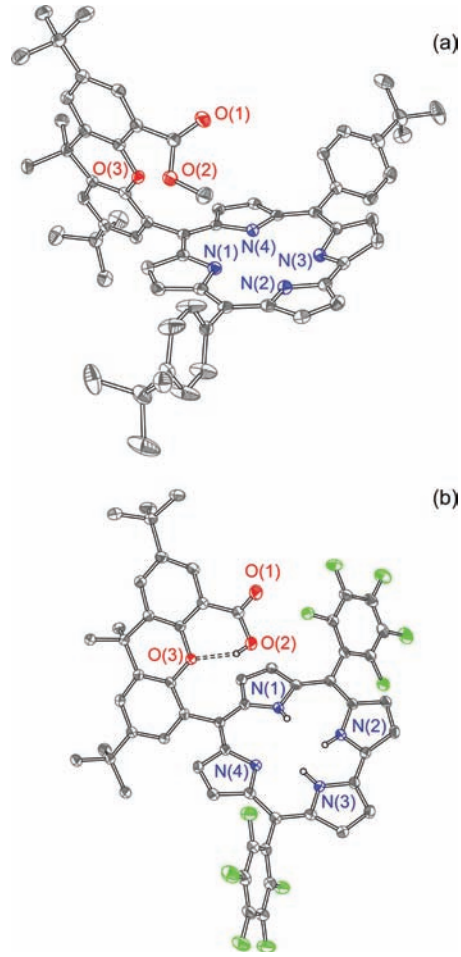

Figure 2. Crystal structures of free base hangman corroles with ester and carboxylic hanging groups (a) **HCX2-CO_2Me** and (b) **HCX1-CO_2H**, respectively. For (a), the hexane solvate molecule and hydrogen atoms are omitted for clarity. Ellipsoids for both structures are depicted at 50% probability level.

for 3 days under nitrogen atmosphere[48] whereas the acidic hydrolysis is performed under even harsher conditions[49] of reflux in a strong acid mixture (sulfuric acid/acetic acid 4:1) for 7 days under nitrogen. We first attempted ester deprotection by basic hydrolysis of HCX-CO_2Me. The reaction gave no product even after the solution was refluxed for 2 weeks under nitrogen atmosphere; only the starting HCX-CO_2Me material was recovered from decomposition products. In an attempt to accelerate the sluggish reactivity associated with the HCX platform, we turned our attention to the application of microwave synthetic methods because we have found it to be effective for the deprotection of hanging ester groups of porphyrins.[50] Basic hydrolysis of the ester group on HCX-CO_2Me under microwave irradiation proceeds within 4−16 h as compared to the several days of the aforementioned conventional thermal hydrolysis conditions. The resulting product was treated with 20% HCl to furnish HCX-CO_2H complexes in high yields for such types of hangman macrocycles (Table 1). A crystal structure of the hydrolyzed freebase hangman corrole **HCX1-CO_2H** shown in Figure 2b is similar to the ester protected hangman complex. The xanthene backbone is tilted relative to the corrole macrocycle but not as much (53° for **HCX1-CO_2H**). The structure of **HCX1-CO_2H** is distinguished by the proton of the carboxylic acid hanging group; an intramolecular hydrogen bond is observed between the carboxylic acid proton and the oxygen of the xanthene backbone, with an observed distance of 2.606(2) Å between the donor and the acceptor oxygen atoms.

The resulting HCX-CO_2H platforms were metalated efficiently (>95%) with $Co(OAc)_2$ using the same conditions as described for the metalation of **1**. The cobalt complexes of HCX-CO_2H were obtained in overall yields of 15 − 20% based on aldehyde **7**.

Spectroscopy and Electronic Structure. The UV−vis absorption spectra of the cobalt hangman corroles offer an interesting comparison to their porphyrin relatives. Figure S14 shows the absorption spectra of the analogous hangman corrole and porphyrin series. The Soret and Q bands of HCX compounds are very broad and exhibit considerably attenuated extinction coefficients as compared to their porphyrin congeners (ca. 50 000 M^{-1} cm^{-1} for CoHCX vs 200 000 M^{-1} cm^{-1} for CoHPX). This asymmetry of the Soret bands is attributed to the lower symmetry of the corrole macrocycle rings.[56] The absence of low-lying d-d states in free-base HCX compounds removes efficient nonradiative decay pathways from the system; consequently, the free base HCX corroles are strongly luminescent (Figures S3d−S6d, S7f and S8f, Supporting Information) at $\lambda_{em,max} \sim 640 - 650$ nm.

A formal electron count involving only the metal does not often adequately account for the electronic structure of corrole complexes, especially when they are highly oxidized. Spectroscopic measurements of highly oxidized corroles are suggestive of a radical cationic state for the corrole macrocycle.[51−56] EPR can be especially helpful in discerning the electron distribution between the metal center and the corrole ligand. The spectroscopic behavior of **1-CoCl** was assessed by X-band EPR spectroscopy using CH_2Cl_2 and THF solution samples, both at cryogenic temperatures in frozen form as well as at room temperature in liquid form. While no signal could be detected at room temperature for fluid solution samples, Figure 3 shows the EPR spectrum of **1-CoCl** recorded at 18 K as a black trace and a simulation of that spectrum is shown by the gray trace. A rhombic signal with a rich hyperfine structure spanning 31 mT is observed. Spectra were recorded at temperatures from 2 to 80 K. At 2 K the observed signal saturates easily, even at 2 μW applied microwave power. For the temperature range where this signal was investigated, its intensity (signal × temperature) was found to be constant, indicating that indeed, the signal arises from an isolated Kramers doublet, as expected for a $S = {}^1/_2$

(48) Chang, C. J.; Yeh, C. Y.; Nocera, D. G. *J. Org. Chem.* **2002**, *67*, 1403–1406.
(49) Rosenthal, J.; Chng, L. L.; Fried, S. D.; Nocera, D. G. *Chem. Commun.* **2007**, 2642–2644.
(50) Dogutan, D. K.; Bediako, D. K.; Teets, T. S.; Schwalbe, M.; Nocera, D. G. *Org. Lett.* **2010**, *12*, 1036–1039.
(51) Cai, S.; Licoccia, S.; D'Ottavi, C.; Paolesse, R.; Nardis, S.; Bulach, V.; Zimmer, B.; Kh; Shokhireva, T.; Walker, F. A. *Inorg. Chim. Acta* **2002**, *339*, 171–178.
(52) Zakharieva, O.; Schünemann, V.; Gerdan, M.; Licoccia, S.; Cai, S.; Walker, F. A.; Trautwein, A. X. *J. Am. Chem. Soc.* **2002**, *124*, 6636–6648.
(53) Cai, S.; Walker, F. A.; Licoccia, S. *Inorg. Chem.* **2000**, *39*, 3466–3478.
(54) Nardis, S.; Paolesse, R.; Licoccia, S.; Fronczek, F. R.; Vicente, M. G. H.; Shokhireva, T. K.; Cai, S.; Walker, F. A. *Inorg. Chem.* **2005**, *44*, 7030–7046.
(55) Walker, F. A.; Licoccia, S.; Paolesse, R. *J. Inorg. Biochem.* **2006**, *100*, 810–837.
(56) Ye, S.; Tuttle, T.; Bill, E.; Simkhovich, L.; Gross, Z.; Thiel, W.; Neese, F. *Chem.—Eur. J.* **2008**, *14*, 10839–10851.

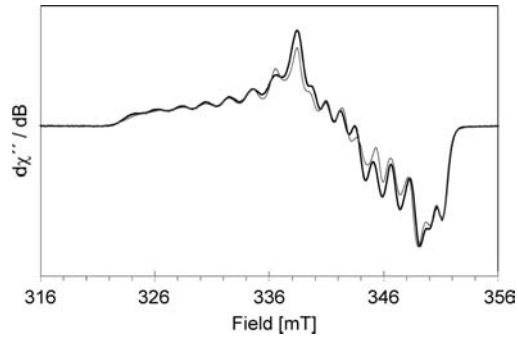

Figure 3. EPR spectrum recorded for **1-CoCl** (black) in THF at 18 K, power 0.2 mW, frequency 9.617 GHz, modulation amplitude 10 G, overlaid with a simulated spectrum (gray) generated using $g_1 = 2.073$, $g_2 = 2.000$, $g_3 = 1.977$ ($\sigma_{g1} = 0.0049$, $\sigma_{g2} = 0.0028$, $\sigma_{g3} = 0.0029$), $A^{Co1} = 58.51$ MHz, $A^{Co2} = 40.23$ MHz, $A^{Co3} = 29.28$ MHz and a Lorentzian line width of 0.0018 mT.

species. Inspection of these spectra reveals the presence, for the low field range, of a clearly defined eight line pattern originating from the hyperfine coupling of the $S = {}^1/_2$ electronic spin to that of the $I = {}^7/_2$ nuclear spin of the ^{59}Co central metal ion. The intricate pattern of the signal for H > 340 mT arises from the overlap of the hyperfine splittings generated by the remaining two components of the hyperfine coupling tensor A^{Co}. The two A tensor components affecting the high and low field regions of the EPR signal can be estimated by evaluating the peak-to-peak separation of the eight line patterns while the remaining component is best determined from spectral simulations. Least square fitting of these spectra using a typical $S = {}^1/_2$ spin-Hamiltonian, eq 1, yielded our best estimates for $g_1 = 2.073$, $g_2 = 2.000$, $g_3 = 1.977$ and $A_1 = 59.0 \pm 1.0$ MHz, $A_2 = 40.0 \pm 1.0$ MHz, $A_3 = 29.5 \pm 0.5$ MHz. Attempts to determine the superhyperfine couplings of the coordinating nitrogen atoms were not conclusive but even if present these couplings would not exceed 3 MHz, a value consistent with the 1.8 − 2.1 MHz range found for [(OEC)Co(C_6H_5)], vide infra. Moreover, the EPR spectra recorded for **1-CoCl** and (TBP)$_8$CzCo(CCSiPh$_3$) are rather similar albeit, with a larger hyperfine splitting pattern observed for the former.[30]

$$\hat{H} = \beta\vec{S}\cdot\tilde{g}\cdot\vec{B} + \sum_k \vec{S}\cdot\tilde{A}^k\cdot\vec{I}_k \qquad (1)$$

In addition to [(TBP)$_8$CzCo(CCSiPh$_3$)], we note that the EPR spectrum of **1-CoCl** also shows a similarity to cobalt(III)-superoxide complexes. We believe that these similarities are due to the analogous electron distributions of the complexes—namely the presence of an unpaired electron delocalized over a noninnocent ligand coordinated to a low-spin cobalt(III) metal ion with the distinction that the unpaired electron for **1-CoCl** and [(TBP)$_8$CzCo(CCSiPh$_3$)] is found mainly in the equatorial plane whereas the unpaired electron is delocalized over the axially coordinated dioxygen moiety of cobalt superoxide complexes. Consequently, for both cases the observed EPR spectra are characterized by g-values that are nearly 2 indicating a lack of spin−orbit interactions and small cobalt hyperfine coupling constants consistent with the assertion that only a small fraction of the spin density is localized over the metal ion. Other observations that do not support the assignment of the EPR spectrum of Figure 3 to an oxygenated cobalt adduct includes: (i) quantification of the observed signal, using a copper spin standard, accounts for the majority of the prepared **1-CoCl** sample, (ii) power saturation and the temperature dependence behaviors of the signal do not reveal the presence of multiple $S = {}^1/_2$ species as it would be expected for a signal arising from a mixture of cobalt oxygenated samples; (iii) the O_2 adducts are difficult to form in the absence of a reductant (vide infra)—bubbling O_2(g) through solutions of **1-Co** for >20 min does not induce changes in the UV−vis and EPR spectra; and finally (v) oxygenated products of **1-CoCl**, [**1-Co**·O_2] (vide infra), display a signal that is distinctly different from that observed for **1-CoCl**, for example, the observed hyperfine splitting pattern spans 31 mT for **1-CoCl** and 46 mT for [**1-Co**·O_2].

The electronic ground state predicted by DFT for the geometry optimized structure of **1-CoCl** is consistent with a redox noninnocent corrole ligand. The ground state is best described as a broken symmetry state with two spin-up, alpha electrons, localized on the central Co(III) ion and one spin-down, beta electron, delocalized on the one-electron oxidized corrole ligand. This state is similar with that determined for the analogous iron-corrole complex, [FeCl(tpfc)], for which the total $S = 1$ ground state is the result of an antiferromagnetic coupling between the $S = {}^3/_2$ of the intermediate-spin Fe(III) site and the $S = {}^1/_2$ of the oxidized corrole ligand.[56] When compared to iron, cobalt complexes are typically found to have a low-spin configuration due to their higher effective nuclear charge, leading to the formation of stronger bonds. However, a quantitative computational investigation of a four-coordinate Co(III)-corrole model, using DFT, predicted a triplet ground state ($S = 1$), ∼2100 cm^{-1} lower in energy than the first excited singlet ($S = 0$) state.[57] Indeed using NMR and SQUID measurements (Figure S2f, Supporting Information), we observe a paramagnetic ground state for **1-Co** in agreement with the theoretical prediction. Moreover, inspection of the magnetic susceptibility data suggests that this complex exhibits a triplet ground state with a large and positive zero field splitting. Considering that for **1-CoCl**, the chloride ion coordinated in the apical position is a weak field ligand, we anticipate the Co(III) ion in this complex to have an intermediate-spin electronic configuration in agreement with the DFT predicted ground state. The predicted values for the magnitudes of the A-tensor components, 370, 108, and 225 MHz, are indicative of two unpaired alpha electrons localized on the Co(III) ion. However, these A values are in stark disagreement with the experimentally observed values. Moreover, the components of both g and A tensors determined for **1-CoCl** are rather similar to those observed for [(OEC)Co(C_6H_5)][58] ($g = 1.967$, 2.112, 2.004; $A^{Co} = 72$, 8, and 10 MHz), a complex that has a single unpaired alpha electron, which is found mainly on the ligand with ∼70% of the spin density delocalized on the corrole ligand and the remaining ∼30% localized on the cobalt ion. For this complex the stabilization of the low-spin electronic configuration for the Co(III) ion is easily rationalized on the basis of the strong σ-donor ligand coordinated in the axial position. The predicted Co−Cl distance for **1-CoCl** of 2.353 Å is found to be 0.11 Å longer than the experimental value of 2.243 Å; this difference is much larger than the 0.04 Å error typically associated with the functional/basis set employed here. An excited state corresponding to a low-spin configuration for the Co(III) ion can be obtained by shortening the Co−Cl distance. By scanning adiabatically along the Co−Cl bond distance we find an energy minimum for this state at 2.233 Å for which the predicted values for the |A|-tensor components of 273, 72, and 33 MHz are

(57) Rovira, C.; Kunc, K.; Hutter, J.; Parrinello, M. *Inorg. Chem.* **2001**, *40*, 11–17.
(58) Harmer, J.; Van Doorslaer, S.; Gromov, J.; Bröring, M.; Jeschke, G.; Schweiger, A. *J. Phys. Chem. B* **2002**, *106*, 2801–2811.

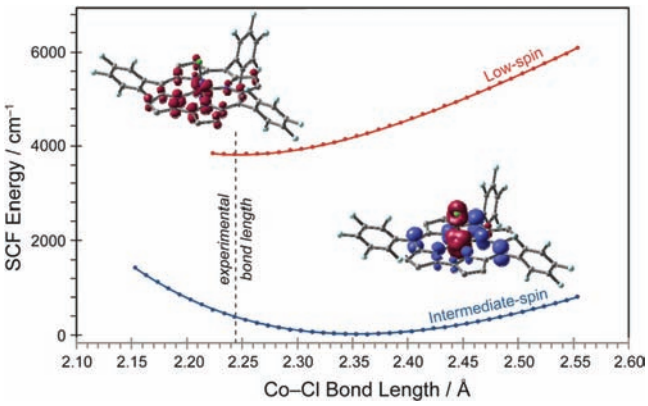

Figure 4. Relative energies of two states of **1-CoCl** for which the Co(III) ion has an intermediate (blue) and low (red) spin electronic configuration; the corresponding surface plots of their spin densities are shown above each curve.

somewhat closer to those experimentally observed. For this excited state we find a single unpaired electron that is delocalized mainly on the corrole ligand (see Figure 4), with a distribution of spin density that is similar to that predicted for [(OEC)Co(C_6H_5)]. Regardless of the electronic configuration of the central cobalt ion, for both states, intermediate and low-spin configurations, we find that the corrole ligand is one-electron oxidized and that the formal Co(IV) center is better described as a Co(III) ion residing within the monocationic radical corrole macrocycle.

Oxygen Reactivity. The hangman effect on the oxygen reduction reaction (ORR) of the Co-HCX series was investigated. Cobalt corroles have been shown to reduce oxygen but the ORR primarily proceeds by the less desirable two-electron energy conversion process to produce hydrogen peroxide; the more desirable four-electron process to produce water is not observed.[19,59−62] Here, ORR activity measurements were made on Co-HCX compounds that were supported on multiwall carbon nanotubes (MWCNTs), which provide a high surface area support for catalysts.[63,64] Table 2 summarizes the electrocatalytic activity as determined from RDE and RRDE measurements of each of the Co-HCX catalysts supported on MWCNT thin film electrodes in acidic solution. The onset for oxygen reduction occurs between 650−700 mV for all of the compounds investigated and the half wave potential for oxygen reduction, $E_{1/2}$, calculated as the potential at which the current equals half the limiting current at 100 rpm, is ∼550 mV vs RHE.

In addition to the potentials at which catalysis occurs, the relative production of water (4 electron reduction) over hydrogen peroxide (2 electron reduction) is also an important factor in assessing activity. The number of electrons transferred during reaction may be extracted from the slope of the Koutecky−Levich plots. For each complex studied the number of electrons transferred is approximately 2 within experimental error, thus

Table 2. Oxygen Reduction by Hangman Corroles Xanthene in Acidic Solution

compound	$E_{1/2}$ (V vs RHE) [b]	n_{avg} [c]	% H_2O_{avg} [d]
1-CoCl	0.56	2.7	40
CoHCX1-CO_2H	0.54	2.9	55
CoHCX1-CO_2Me	0.58	2.6	30
CoHCX2-CO_2H	0.52	2.5	25
CoHCX3-CO_2H	0.56	2.8	41

[a] Determined from data shown in Figures S15 to S19 (Supporting Information). [b] $E_{1/2}$, calculated as the potential at which the current equals half the limiting current at 100 rpm. [c] n = number of electrons as calculated from RRDE data according to $4I_d/(I_d + (I_r/N))$. [d] %H_2O produced during ORR as calculated from RRDE data according to $(2I_r/N)/(I_d + (I_r/N))$ where I_r = ring current, I_d = disk current, and N = collection efficiency.

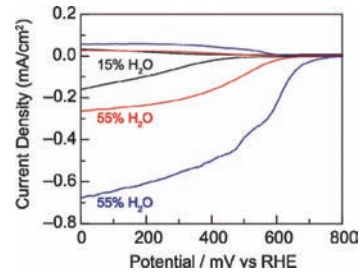

Figure 5. RRDE of edge-plane-graphite disk (black), **CoHCX1-CO_2H** on EPG disk (red), and **CoHCX1-CO_2H** on MWCNTs (blue) in 0.5 M H_2SO_4 at 100 rpm. Disk current (negative) and Pt ring current (positive). Scan rate 20 mV/s.

suggesting reduction to hydrogen peroxide. However, a more precise measure of the ratio between hydrogen peroxide and water may be made based on the RRDE data (Table 2), which directly measures the amount of peroxide generated. The parent complex **1-CoCl** reduces oxygen with lower selectivity than the hangman corrole congeners. ORR by **1-CoCl** is primarily to hydrogen peroxide consistent with previous studies in acidic and pH 7 solution where peroxide was also observed as the major product for this molecule.[19,61] The hangman effect is best demonstrated by comparison of RRDE data for ORR activity between **CoHCX1-CO_2Me** and **CoHCX1-CO_2H**; in the absence of a proton on the hanging group, selective reduction of oxygen to water drops by 25%. This result highlights the importance that the hanging group be able to transfer a proton in order to promote O−O bond cleavage.

To ensure that immobilization on the MWCNT film did not affect the ORR mechanism of the corrole ORR catalysis, we undertook ORR measurements on **CoHCX1-CO_2H** immobilized on EPG and MWCNT electrodes. Figure 5 shows the ORR activity at 100 rpm for EPG, **CoHCX1-CO_2H** on EPG, and **CoHCX1-CO_2H** supported on MWCNTs. Under similar experimental conditions, the percent water formed for **CoHCX1-CO_2H** films on MWCNT and on EPG is the same. However, ORR activity of the corrole catalyst on MWCNT occurs at a lower onset potential with higher current density. This behavior has been seen previously for porphyrins[9] and is consistent with a higher loading of catalyst per geometric surface area afforded by the MWCNT support.

Activity is highest for each complex at the potential corresponding to the $E_{1/2}$. Similar to results for asymmetrically substituted corroles without a hanging group, the $E_{1/2}$ does not shift significantly among the CoHCX series, indicating that the substitution pattern does not play a significant role in shifting the activity of the molecules.[19] Previous results with porphyrin macrocycles have indicated that the activity is improved when the macrocycle is

(59) Kadish, K. M.; Fremond, L.; Ou, Z. P.; Shao, J. G.; Shi, C. N.; Anson, F. C.; Burdet, F.; Gros, C. P.; Barbe, J. M.; Guilard, R. *J. Am. Chem. Soc.* **2005**, *127*, 5625–5631.
(60) Kadish, K. M.; Frémond, L.; Burdet, F.; Barbe, J.-M.; Gros, C. P.; Guilard, R. *J. Inorg. Biochem.* **2006**, *100*, 858–868.
(61) Collman, J. P.; Kaplun, M.; Decreau, R. A. *Dalton Trans.* **2006**, 554–559.
(62) Givaja, G.; Volpe, M.; Edwards, M. A.; Blake, A. J.; Wilson, C.; Schroder, M.; Love, J. B. *Angew. Chem., Int. Ed.* **2007**, *46*, 584–586.
(63) Choi, A.; Jeong, H.; Kim, S.; Jo, S.; Jeon, S. *Electrochim. Acta* **2008**, *53*, 2579–2584.
(64) Qu, J.; Shen, Y.; Qu, X.; Dong, S. *Electroanalysis* **2004**, *16*, 1444–1450.

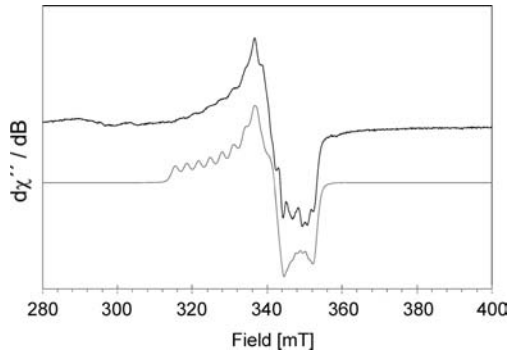

Figure 6. CW X-band EPR spectrum of [**1-Co**•O_2] recorded at 20 K, microwave power 2 mW, modulation amplitude 10 G, frequency 9.631 GHz (black) and simulation (gray) obtained for an $S = {}^1/_2$ using $g_1 = 2.113$, $g_{2,} = 2.017$, $g_3 = 1.979$, with g-strain such that $\sigma_{g1} = 0.007$, $\sigma_{g2} = 0.004$, $\sigma_{g2} = 0.006$; an A tensor such that $A_1 = 93.2$ MHz, $A_2 = 29.1$ MHz, $A_3 = 35.7$ MHz and Euler angles that account for the rotation of the A vs g tensor $\alpha = 12°$, $\beta = 9°$ and $\gamma = 0°$.

electron deficient, and within the CoHCX series, the highest activity is indeed observed for **CoHCX1-CO_2H**.

Insight into the mechanism for ORR comes from a comparison of the EPR signals from the Co corrole platform in the presence and absence of oxygen under reducing conditions. Although the NMR spectra and SQUID measurement (see Figure S2f, Supporting Information) indicate that **1-Co** has a paramagnetic triplet ground state, since it is an integer spin, not a Kramers system, we do not expect to observe an EPR signal in transversal mode at X-band. Indeed, spectra recorded at cryogenic temperatures from 2 to 100 K for a frozen THF solution sample of **1-Co** show only the presence of a heterogeneous, axial, $S = {}^1/_2$ signal that accounts for less than 1% of the total cobalt amount in the sample (Figure S2g, Supporting Information). Addition of an ethanol solution containing excess $NaBH_4$ to this **1-Co** sample does not result in the appearance of an EPR signal that could be associated with a homogeneous Co(II) species (Figure S2g, Supporting Information). However, electronic absorption spectra clearly show that the cobalt center is reduced. The forest green solution turns yellow green upon the addition of $NaBH_4$; the Soret and Q-bands decrease in intensity with the concomitant appearance of a new band at 990 nm (Figure S2h, Supporting Information). The reduction product does not change even with the addition of up to a 10 equivalent excess of reducing agent. Exposure of this solution to O_2(g) results in the restoration of the Soret and Q-band intensities that are characteristic of an oxidized cobalt center. Fast freezing of O_2(g) exposed solutions of the reduced cobalt corrole macrocycle leads to the EPR spectrum displayed in Figure 6, which exhibits an intense $S = {}^1/_2$ rhombic signal with an apparent ^{59}Co hyperfine splitting. This finding indicates that in the presence of a strong reductant such as $NaBH_4$, **1-Co** binds O_2 even though no stabilizing base, for example, pyridine, is present. This signal was investigated at temperatures from 2 to 80 K. In addition to the $g \approx 2$ signal associated with the [**1-Co**•O_2] adduct under various experimental conditions a very broad signal with resonances at 4.6, 1.6, and 1.4 is observed. The latter signal originates from a high-spin heterogeneous Co(II) species, most likely, the result of a decomposition process. Spin quantification of the $g \approx 2$ signal using a copper standard and spectral simulations indicate that this species accounts for ~80% of the total metal content. The spectra recorded for [**1-Co**•O_2] are rather similar in appearance to those observed for the dioxygen-[(corrolazine)Co(py)] adduct and of other mononuclear cobalt(II)−O_2 complexes.[30,65−68]

Overall, the CoHCX series operates under a mixed 2-electron/4-electron mechanism. The activity of the series appears to be dominated by the electronic properties of the macrocycle core and peripheral substitution offers more modest changes in reactivity as compared to porphyrin analogues. The installation of a proton-donating moiety over the face of the macrocycle results in enhanced ORR activity for CoHCX corrole complexes, promoting the four-electron pathway.

Conclusion

Hangman cobalt corroles are a new ligand scaffold for PCET catalysis that are synthesized in good yields from a one-pot condensation of dipyrromethane with the aldehyde of a xanthene spacer followed by metal insertion using microwave irradiation. Spectroscopic investigation of the cobalt corroles axially ligated by chloride using X-band EPR support the description of a [Co(III)Cl-corrole$^{+\bullet}$] in which the corrole ligand is redox noninnocent. These higher oxidation state species are important in small molecule activation reactions involving O−O bond cleavage.[69] Along these lines, the hangman corroles promote ORR. The hangman corroles are distinguished from their unmodified counterparts by the presence of an intramolecular proton transfer network, which is able to couple to redox processes occurring at the corrole platform. We show here for ORR that the proton-donating hanging group works in concert with the corrole platform to activate the O−O bond.

Acknowledgment. We acknowledge Lee-Ping Wang for useful discussions on computational chemistry and Dr. Danna Freedman for collecting the magnetic susceptibility data of **1-CoCl**. The developments of new synthetic methods and synthesis of the new compounds were performed under the sole sponsorship of Eni S.p.A under the Eni-MIT Alliance Solar Frontiers. EPR spectra were recorded at Carnegie Mellon University, in Prof. Eckard Münck laboratory; this research has been supported by the U.S. NIH (EB001475 to E.M.). S.A.S. thanks Prof. Emile Bominaar for useful discussions. Program and characterization work was executed under the Division of Chemical Sciences, Geosciences, and Biosciences, Office of Basic Energy Sciences of the U.S. Department of Energy through Grant DE-FG02-05ER15745. M.S. thanks the German Academic Exchange Service (DAAD) for fellowship support within the Postdoc-Programme. T.S.T. acknowledges the Fannie and John Hertz Foundation for a graduate research fellowship.

Supporting Information Available: Full experimental details for synthesis, NMR, MALDI-MS and high resolution ESI-MS spectral data of corrole compounds, crystallographic data, electronic spectra, CVs, computational details, and ORR RDE and RRDE traces. This material is available free of charge via the Internet at http://pubs.acs.org.

JA108904S

(65) Hoffman, B. M.; Diemente, D. L.; Basolo, F. *J. Am. Chem. Soc.* **1970**, *92*, 61–65.
(66) Walker, F. A. *J. Am. Chem. Soc.* **1970**, *92*, 4235–4244.
(67) Van Doorslaer, S.; Schweifer, A. *J. Phys. Chem. B.* **2000**, *104*, 2919–2927.
(68) Jörin, E.; Schweiger, A.; Günthard, Hs. H. *Chem. Phys. Lett.* **1979**, *61*, 228–232.
(69) Kim, S. H.; Park, H.; Seo, M. S.; Kubo, M.; Ogura, T.; Klajn, J.; Gryko, D. T.; Valentine, J. S.; Nam, W. *J. Am. Chem. Soc.* **2010**, *132*, 14030–14032.